RSC Advances

PAPER

View Article Online
View Journal | View Issue

Cite this: *RSC Adv.*, 2019, **9**, 29873

$CoFe_2O_4/Cu(OH)_2$ magnetic nanocomposite: an efficient and reusable heterogeneous catalyst for one-pot synthesis of β-hydroxy-1,4-disubstituted-1,2,3-triazoles from epoxides†

Ronak Eisavi * and Asmar Karimi

Received 3rd August 2019
Accepted 13th September 2019

DOI: 10.1039/c9ra06038c

rsc.li/rsc-advances

A magnetically separable $CoFe_2O_4/Cu(OH)_2$ nanocomposite was prepared and characterized by various techniques such as FESEM, EDS, TEM, XRD, VSM and FT-IR. This novel composite was used as a heterogeneous catalyst for the regioselective synthesis of β-hydroxy-1,4-disubstituted-1,2,3-triazoles from sodium azide, terminal alkynes and structurally different epoxides in water at 60 °C. The formation of the product proceeds in one pot through a mechanism that involves an *in situ* generated organic azide intermediate, followed by rapid ring closure with the alkyne component. The simple procedure, short reaction times, perfect regioselectivity, high product yields, and use of a benign solvent and nontoxic catalyst are among the considerable advantages of this protocol. Furthermore, the catalyst was easily separated using an external magnet and reused several times without any significant loss of catalytic activity or magnetic properties.

1. Introduction

1,2,3-Triazoles are significant heterocyclic intermediates for the manufacture of important compounds such as pharmaceuticals, agrochemicals, dyes and corrosion retarding agents.[1–4] They also show vital biological activities such as anticancer,[5] anti HIV,[6] antiviral, antiallergic,[7] antifungal,[8] antibacterial,[9] antitubercular,[10] anti-inflammatory,[11] antimalarial,[12] and antioxidant activities.[13]

The Huisgen 1,3-dipolar cycloaddition of alkynes and organic azides has been developed as the principal method for synthesis of 1,2,3-triazoles.[14–22] Recently, multicomponent one-pot synthesis of β-hydroxy-1,2,3-triazoles has been carried out through *in situ* click reaction of azides, alkynes and epoxides in the presence of heterogeneous copper catalysts such as carbon supported copper nanoparticles,[23,24] porphyrinatocopper nanoparticles,[25] $CuSO_4 \cdot 5H_2O$/sodium ascorbate,[26] copper(I)-zeolite,[27] Cu[N^2,N^6-bis(2-hydroxyphenyl)pyridine-2,6-dicarboxamidate]/ascorbic acid,[28] copper ferrite nanoparticles,[29] copper(I)@phosphorated SiO_2,[30] $Cu(OAc)_2 \cdot H_2O$,[31] (Cu/Cu_2O) nanoparticles,[32] Cu(II)-azide complexes,[33] Cu(II)-DA@nano $AlPO_4$,[34] 1,4-dihydroxyanthraquinone-copper(II) nanoparticles immobilized on silica gel,[35] 4′-phenyl-2,2′:6′,2″-terpyridine copper(II) complex immobilized on activated multiwalled carbon nanotubes,[36] CuI[37] and $NiFe_2O_4$-glutamate-Cu.[38] Ramachary–Bressy–Wang cycloaddition of enolate intermediates and organic azides is the other basic method for one-pot preparation of 1,4-disubstituted-1,2,3-triazoles.[39–43]

The reduction of work-up procedures and purification steps, high purity of desired products, short reaction times, high to excellent yields are among the significant benefits of multicomponent one-pot reactions.[44,45] Furthermore, the reaction involving ring opening of epoxides with organic azides in water solvent occurs with perfect regioselectivity and takes advantage of green and benign conditions.

In recent years, magnetic nanoparticles (MNPs) due to their facile preparation, easy separation using an external simple magnet leading to avoid traditional filtration processes, recoverability and reusability,[46,47] high catalytic activity,[48] thermal and chemical stability[49,50] have been widely utilized as green and efficient nanocatalysts in the synthesis of organic compounds. Nevertheless, the nano-ferrites often suffer from high tendency of self-aggregation and low quantity of functional groups on the surface.[51,52] The coating of nano-ferrites with a functionalized shell, not only reduces the aggregation of the nanoparticles in the solution, but also improves the efficiency of the catalyst by increasing the amount of functional groups on the surface.[53] Recently, these coated nanostructures have received special attention as air-stable materials and easy separable catalysts in organic transformations, drug targeting, and magnetic cell separation.[54–57]

In connection with our recent works on nano-ferrites,[58–63] herein we wish to report an efficient one-pot three-component

Department of Chemistry, Payame Noor University, PO BOX 19395-3697, Tehran, Iran. E-mail: roonak.isavi@gmail.com

† Electronic supplementary information (ESI) available: Spectral data for β-hydroxy-1,2,3-triazoles. See DOI: 10.1039/c9ra06038c

protocol for the synthesis of β-hydroxy-1,2,3-triazoles from sodium azide, terminal alkynes, and various epoxides in the presence of $CoFe_2O_4/Cu(OH)_2$ magnetic nanoparticles as a novel and green heterogeneous catalyst in water (Scheme 1).

2. Experimental

2.1. Instruments and materials

All materials were purchased from the Merck and Aldrich Chemical Companies with the best quality and they were used without further purification. The synthesized nanocatalyst was characterized by XRD on a Bruker D8-Advanced diffractometer with graphite-monochromatized Cu Kα radiation ($\lambda = 1.54056$ A°) at room temperature. Magnetic property of synthesized nanocatalyst was measured using a VSM (Meghnatis Daghigh Kavir Co., Kashan Kavir, Iran) at room temperature. TEM image was recorded using an EM10C-100 kV series microscope from the Zeiss Company, Germany. FESEM images were determined using FESEM-TESCAN. The energy dispersive X-ray spectrometer (EDS) analysis was taken on a MIRA3 FE-SEM microscope (TESCAN, Czech Republic) equipped with an EDS detector (Oxford Instruments, UK). IR and $^1H/^{13}C$ NMR spectra were recorded on Thermo Nicolet Nexus 670 FT-IR and 400 MHz Bruker Avance spectrometers, respectively. The products were characterized by their spectra data and comparison with the reported data in literature. All yields refer to isolated pure products.

2.2. Preparation of $CoFe_2O_4$ nanoparticles

$CoFe_2O_4$ nanoparticles were prepared by a solid-state procedure according to our previous research.[58] Briefly, in a mortar, $CoCl_2$, $Fe(NO_3)_3 \cdot 9H_2O$, NaOH, and NaCl were mixed with the desired molar ratio (1 : 2 : 8 : 2) and ground together for 55 min. The reaction started quickly along with the release of heat. The mixture color changed from yellow to chocolate brown after 4 min. Next, in order to remove the additional salts, the produced mixture was washed with distilled water for several times. The product was dried at 80 °C for 2 h and it was then calcined at 900 °C for 2 h to obtain the final cobalt nanoferrite as a dark brown powder.

2.3. Synthesis of $CoFe_2O_4/Cu(OH)_2$ nanocomposite

In a round-bottomed flask equipped with a magnetic stirrer, a solution of $CuCl_2 \cdot 2H_2O$ (0.8 g, 4.7 mmol) in distilled water (30 mL) was prepared and then $CoFe_2O_4$ (1.01 g, 4.31 mmol) was added. The mixture was stirred vigorously for 10 min at room temperature and followed by dropping of NaOH solution (6 mL, 1 M) in order to basify the mixture up to pH ~ 13. The stirring of alkali mixture was continued at room temperature for 24 h. The black nanoparticles of $CoFe_2O_4/Cu(OH)_2$ were separated using a magnet, washed with distilled water and then dried under air atmosphere within two days.

2.4. One-pot synthesis of β-hydroxytriazoles from epoxides catalyzed by $CoFe_2O_4/Cu(OH)_2$ in water: a general procedure

In a round-bottomed flask equipped with a magnetic stirrer and condenser, a solution of the epoxide (1 mmol), alkyne (1 mmol) and sodium azide (0.078 g, 1.2 mmol) in H_2O (5 mL) was prepared. $CoFe_2O_4/Cu(OH)_2$ nanocomposite (0.032 g, 0.1 mmol) was then added to the solution and the resulting mixture was stirred magnetically for 3–6.5 h at 60 °C. The progress of the reaction was monitored by TLC using CCl_4 : Et_2O (10 : 2) as an eluent. After completion of the reaction, the magnetic nanocatalyst was separated using an external magnet and collected for the next run. The reaction mixture was extracted with EtOAc (3 × 10 mL) and then dried over anhydrous Na_2SO_4. After evaporating the organic solvent, the crude β-hydroxytriazoles were obtained. Removal of the solvent under vacuum, followed by recrystallization with EtOH/H_2O (3 : 1) or purification on

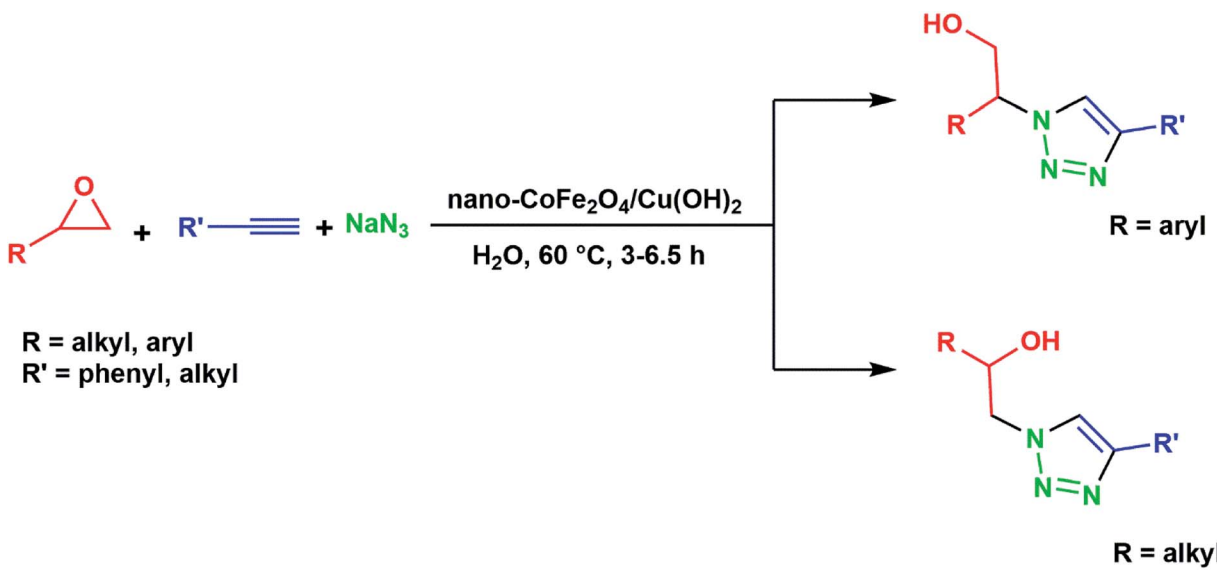

Scheme 1 One-pot synthesis of triazoles from epoxides catalyzed by $CoFe_2O_4/Cu(OH)_2$ nanoparticles.

silica gel using CCl_4 : Et_2O (10 : 2) as the eluent afforded the pure β-hydroxytriazoles derivatives in 75–95% yield (Table 2). The collected $CoFe_2O_4/Cu(OH)_2$ nanoparticles were washed with distilled water and dried for the next cycle. All products are known compounds and were characterized by comparison of their spectra (FT-IR, ^1H NMR and ^{13}C NMR) with those of valid samples;[23,25,26,29,30,38,45] these data are given in the ESI.†

3. Results and discussion

3.1. Synthesis and characterization of $CoFe_2O_4/Cu(OH)_2$ magnetic nanocatalyst

The coating of $CoFe_2O_4$ nanoparticles was carried out with $Cu(OH)_2$ in order to reduce the self-aggregation and also increase the amount of hydroxyl functional groups on the surface of nano-ferrite which makes the catalyst more active than the bare cobalt ferrite. The use of $CoFe_2O_4$ nanoparticles as catalyst support not only donated sufficient magnetic property for the easy separation of nanocatalyst, but also enhanced the efficiency of the catalyst by increasing the recoverability and reusability of the novel nanocomposite.

The magnetic nanoparticles of $CoFe_2O_4/Cu(OH)_2$ was synthesized in a two-step process. $CoFe_2O_4$ was prepared using solid-state reaction of $CoCl_2$, $Fe(NO_3)_3{\cdot}9H_2O$, NaCl and NaOH in an agate mortar (Scheme 2). After calcination of crude powder at 900 °C, the $CoFe_2O_4$ nanoparticles were obtained with high crystallinity, phase purity and increased saturation magnetization (M_s). The calcination process at high temperatures improves the efficiency of $CoFe_2O_4$, and also leads to decompose the excess salts used in the preparation of these nanoparticles.[64] Afterwards, the collected pure $CoFe_2O_4$ nanoparticles were added to an aqueous solution of $CuCl_2$ and followed by dropping of the NaOH solution under intense stirring. Eventually, the black precipitate was accumulated through magnetic separation, washed with deionized water, and dried at room temperature (Scheme 3). The prepared $CoFe_2O_4/Cu(OH)_2$ nanocatalyst was characterized by vibration sample magnetometer (VSM), FT-IR, X-ray diffraction (XRD), transmission electron microscopy (TEM), field emission scanning electron microscope (FESEM), and energy dispersive X-ray spectrometer (EDS) techniques.

3.1.1. Vibration sample magnetometer (VSM). The hysteresis loops, saturation magnetization (M_s) and switching field (H_c) of the prepared magnetic nanoparticles were measured at room temperature using vibrating sample magnetometer. The hysteresis loops of $CoFe_2O_4$ and $CoFe_2O_4/Cu(OH)_2$ nanoparticles are shown in Fig. 1. The wide cycles and the hysteresis loops show the behavior of hard ferromagnetic particles with high coercivity. $CoFe_2O_4/Cu(OH)_2$ nanoparticles show lower magnetization saturation (18 emu g^{-1}) than the uncoated cobalt ferrite nanoparticles (128 emu g^{-1}). This is due to the effect of $Cu(OH)_2$ shell coating where each particle was separated from its neighbors by the coated layer leading to decrease the magnetostatic coupling between the particles.

3.1.2. Fourier transform infra-red (FT-IR) spectrum. The FT-IR spectrum of synthesized $CoFe_2O_4$, $Cu(OH)_2$ and $CoFe_2O_4/Cu(OH)_2$ nanoparticles are shown in Fig. 2. A strong absorption band at 596 cm^{-1} is corresponded to the stretching vibration of metal–oxygen (M–O) indicating the formation of spinel ferrite structure. The absorption peaks at 1608 cm^{-1} and 3390 cm^{-1} are related to bending and stretching vibrations of O–H group in surface absorbed H_2O in the sample, respectively.[65] A sharp and intense absorption band at 3568 cm^{-1} is related to the O–H stretching vibrations in crystal structure of $Cu(OH)_2$ and the peak at 941 cm^{-1} indicates Cu–O–H bending vibrations.[66]

3.1.3. X-ray diffraction (XRD). Fig. 3 displays the X-ray diffraction (XRD) patterns of $CoFe_2O_4$, $Cu(OH)_2$ and $CoFe_2O_4/Cu(OH)_2$ nanoparticles. In the XRD pattern of $CoFe_2O_4/Cu(OH)_2$, all the peaks of $CoFe_2O_4$ and $Cu(OH)_2$ are detectable. The lines (111), (220), (311), (222), (400), (422), (511), (440), (620), (533) and (622) related to 2θ = 18.36°, 30.18°, 35.54°, 37.18°, 43.17°, 53.55°, 57.09°, 62.68°, 71.13°, 74.13° and 75.20° respectively, are assigned to the diffraction of $CoFe_2O_4$ crystals and indicate that the synthesized $CoFe_2O_4$ nanoparticles are pure and high crystalline. These peaks are consistent with the standard data (JCPDS card no. 22-1086).[67] The peaks at 2θ = 16.81°, 23.89°, 34.09°, 38.24°, and 39.77° correspond to orthorhombic $Cu(OH)_2$ which are in good agreement with JCPDS no. (13-420).[68] The peak at 53.52° for copper hydroxide overlaps with the 53.55° peak of $CoFe_2O_4$. The average crystallite size of $CoFe_2O_4/Cu(OH)_2$ nanoparticles is calculated using the Scherrer's formula (40 nm).

3.1.4. TEM, FESEM and EDS of $CoFe_2O_4/Cu(OH)_2$ nanocomposite. The morphology and size distribution of the synthesized nanocatalyst have been investigated by TEM and FESEM techniques. Fig. 4 shows the TEM images of the $CoFe_2O_4/Cu(OH)_2$ nanocomposite. The TEM images with different magnifications clearly reveal the wire shape of the

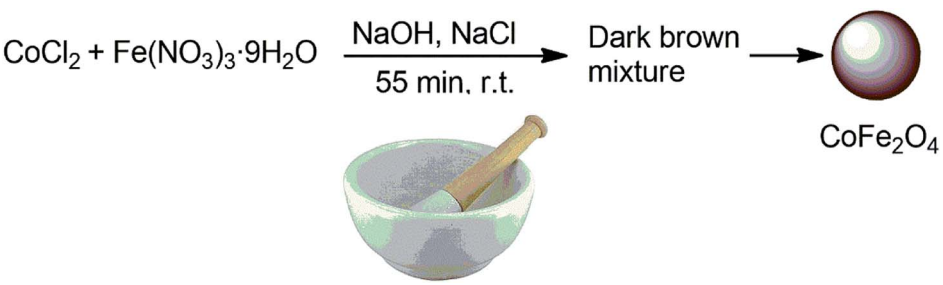

Scheme 2 Synthesis of $CoFe_2O_4$ nanoparticles.

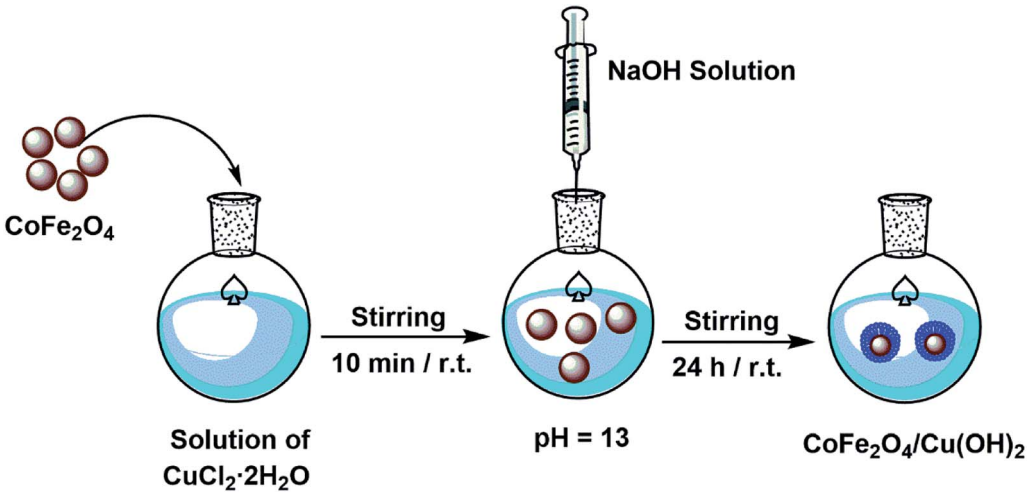

Scheme 3 Synthesis of $CoFe_2O_4/Cu(OH)_2$ nanocomposite.

$Cu(OH)_2$ nanoparticles, and also show that many nanowires come together to form a bundle-like morphology. The $CoFe_2O_4$ nanoparticles are spherical and have been uniformly surrounded by $Cu(OH)_2$ nanowires, indicating the successful coating of $CoFe_2O_4$ surface with $Cu(OH)_2$. The images also demonstrated that the agglomeration of $CoFe_2O_4$ nanoparticles has not occurred. The cobalt ferrite particles are clearly distinguishable as black spherical segments with diameter 40 nm. The gray particles of $Cu(OH)_2$ are also obviously detectable in TEM images.

The FESEM images confirm the nanowire structure of the catalyst containing the spherical cobalt ferrite nanoparticles, and show that the diameter of wires lies in the range of 28 to 40 nm. Each nanobelt with an average diameter of 32 nm is composed of tiny nanostructured grains that were created during the reaction in solution but has a uniform shape (Fig. 5). The obtained results are in good agreement with TEM and XRD data.

The chemical composition of $CoFe_2O_4/Cu(OH)_2$ was approved with EDS analysis. In this analysis, Cu, Co, Fe, and O signals are detectable (Fig. 6).

3.1.5. Structure of $CoFe_2O_4/Cu(OH)_2$ nanocomposite. The possible structure of $CoFe_2O_4/Cu(OH)_2$ nanocomposite was proposed based on the characterization results (Scheme 4). In the presented catalytic system, copper plays the key role in the [3 + 2] cycloaddition between alkyne and azide components, and the use of nano-$CoFe_2O_4$ as a magnetic support facilitates the separation, accumulation and recycling of nanoparticles.

3.2. Catalytic activity of $CoFe_2O_4/Cu(OH)_2$ for the synthesis of 1,4-disubstituted β-hydroxy-1,2,3-triazoles

The optimization of reaction conditions was conducted with styrene oxide, phenylacetylene and sodium azide as a model reaction. The quantity of catalyst, temperature, time and solvents were investigated as the main optimization factors

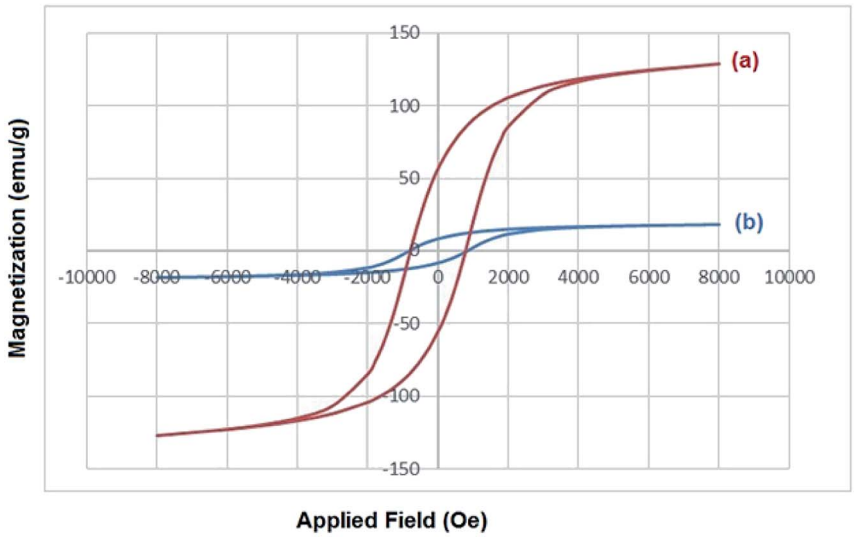

Fig. 1 Magnetization curves of (a) $CoFe_2O_4$ (b) $CoFe_2O_4/Cu(OH)_2$ nanoparticles.

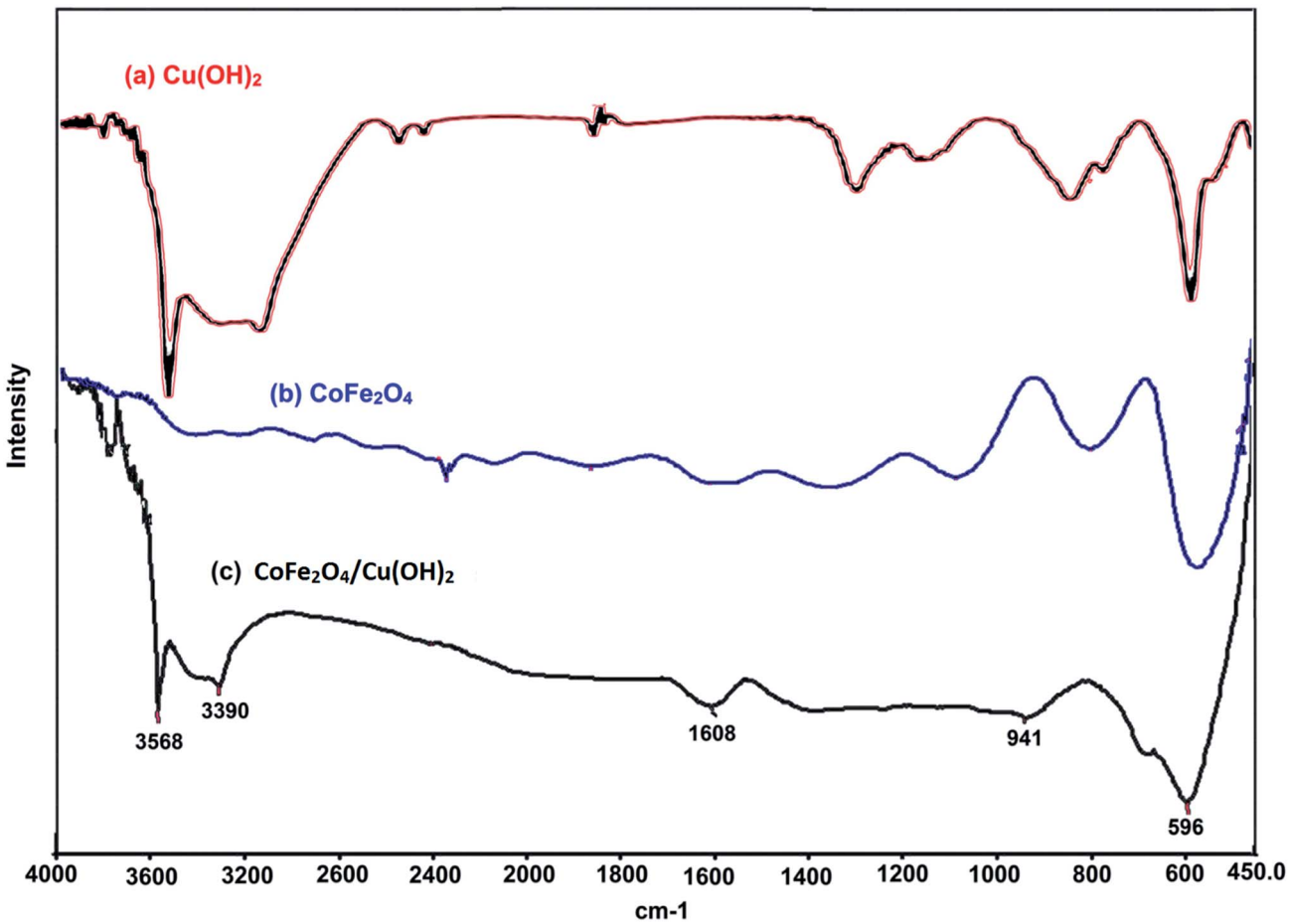

Fig. 2 FT-IR (KBr) spectrum of (a) $Cu(OH)_2$, (b) $CoFe_2O_4$ and (c) $CoFe_2O_4/Cu(OH)_2$.

(Table 1). The desired result was obtained using styrene oxide (1 mmol), phenylacetylene (1 mmol) and sodium azide (1.2 mmol) in the presence of $CoFe_2O_4/Cu(OH)_2$ (0.032 g, 0.10 mmol, 10 mol%) in water at 60 °C (entry 5). As can be seen, the use of catalytic amount of nanocatalyst was essential to perform the reaction and in the absence of catalyst, no cyclization product was generated after 10 h (entry 1). The model reaction was tested using the various amounts of $CoFe_2O_4/Cu(OH)_2$ (0.01, 0.02, 0.025, 0.032 and 0.045 g), and the best result was achieved using (0.032 g) of catalyst (entries 2–6). The enhancement of catalyst amount from 0.01 to 0.032 g, not only increased the reaction speed, but also led to raise the product yield significantly. Applying the more amounts of nanocatalyst did not ameliorate the product yield (entry 6).

The effect of solvents was also studied by performing the cyclization reaction in various solvents. It was observed that the reaction was carried out in polar solvents, such as water, ethanol, acetonitrile, ethyl acetate, methanol and dimethylformamide whereas no reaction took place in nonpolar solvents (entries 7–13). The reaction was accomplished efficiently in H_2O and in comparison with water, the product yields were lower in all other solvents; hence, this solvent was selected as a green and eco-friendly option for synthesis of triazoles.

In order to determine the effect of temperature, the reaction was repeated at different temperatures (25 °C, 40 °C and 60 °C). At room temperature (25 °C), the reaction was carried out in 8 h affording the moderate yield of product (entry 14). But increasing the temperature encouragingly raised both the product yield and reaction speed, and the corresponding triazole was prepared in 65% yield after 5 h at 40 °C (entry 15). With further increase in temperature to 60 °C the yield increased to 94% after 3.3 h (entry 5).

Performing the mentioned reaction under the optimized conditions but in the presence of $CoFe_2O_4$ (without the copper hydroxide) produced a trace of the corresponding triazole after 5 h (entry 16). Cobalt ferrite without $Cu(OH)_2$ was not capable of conducting the reaction. The reaction was also investigated using bare $Cu(OH)_2$ nanoparticles under the same conditions (entry 17). The reaction was carried out within 3.5 h giving 90% yield of product. The presence of copper hydroxide significantly enhanced the catalytic capability. These results approved the essential catalytic role of copper hydroxide particles. It also showed that the interactions between the $Cu(OH)_2$ and $CoFe_2O_4$ nanoparticles may increase the catalytic activity of $CoFe_2O_4/Cu(OH)_2$ composite. Cobalt ferrite plays the role of a magnetic support that enhances the effectiveness of the catalyst by increasing the contact surface and easy separability.

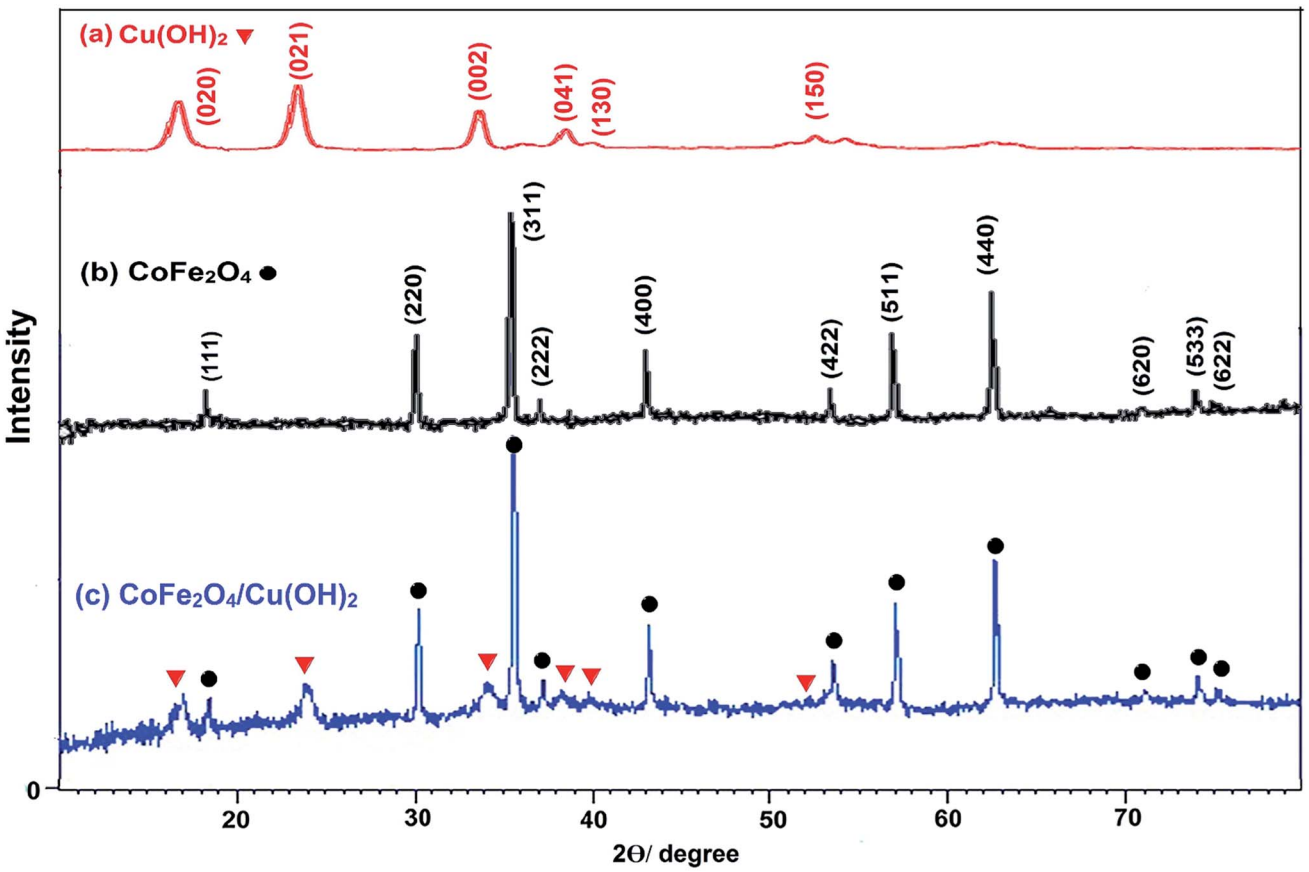

Fig. 3 The X-ray diffraction patterns of (a) nano-$Cu(OH)_2$, (b) nano-$CoFe_2O_4$ and (c) $CoFe_2O_4/Cu(OH)_2$ nanocomposite.

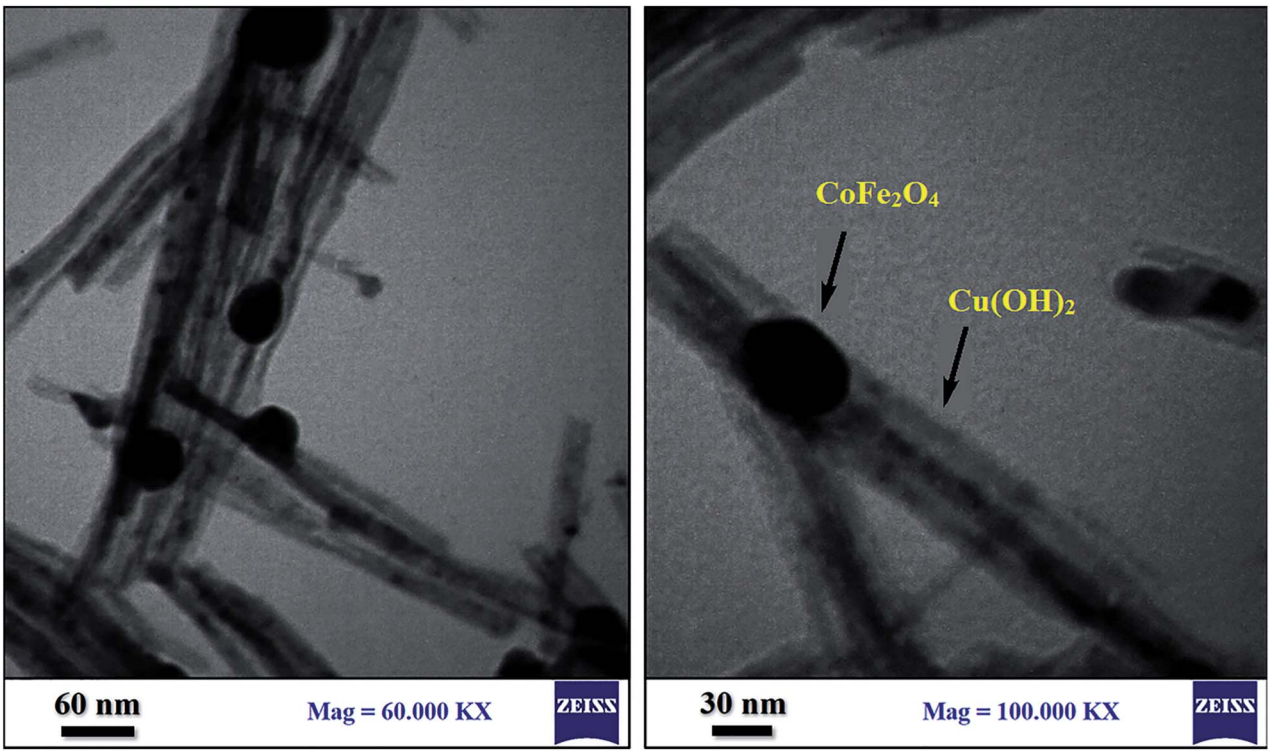

Fig. 4 TEM images of $CoFe_2O_4/Cu(OH)_2$.

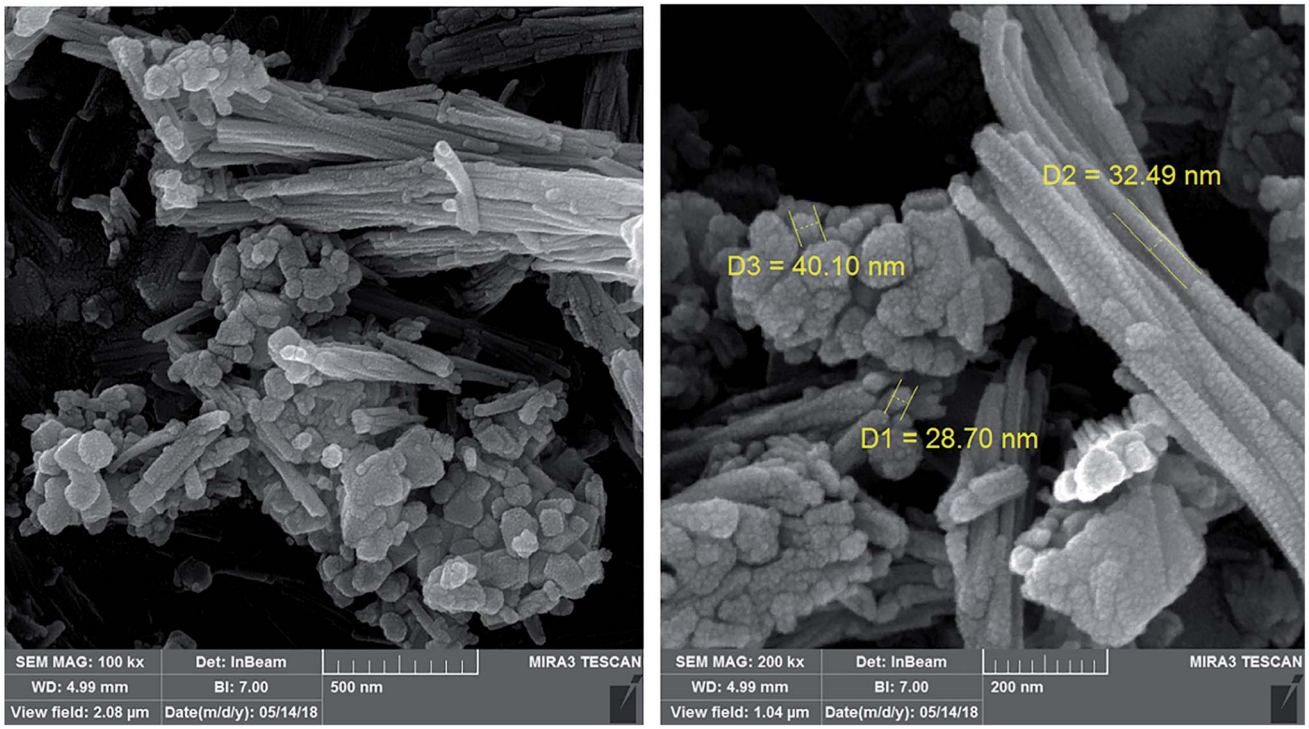

Fig. 5 FESEM images of $CoFe_2O_4/Cu(OH)_2$.

In order to exhibit the diversity of the $CoFe_2O_4/Cu(OH)_2$ catalyst, the optimized conditions were applied to epoxides containing either electron-donating or -withdrawing substituents, and cyclic epoxides as shown in Table 2. In addition, the reaction of aliphatic terminal alkynes with styrene oxide was also considered under mentioned conditions (entries 18–21). All reactions were carried out successfully within 3–6.5 h to give 1,2,3-triazoles in 75–95% yields.

3.3. Recycling of $CoFe_2O_4/Cu(OH)_2$ nanoparticles

The recyclability of nano-$CoFe_2O_4/Cu(OH)_2$ was investigated in the synthesis of 3-chloro-1-(4-phenyl-1*H*-1,2,3-triazol-1-yl) propan-2-ol as halogen containing sample (Table 2, entry 15) and 2-hydroxy-3-(4-phenyl-1*H*-1,2,3-triazol-1-yl)propyl methacrylate with the lowest yield in the first run (Table 2, entry 7). After completion of the reaction, the reaction mixture was cooled to room temperature and the nanoparticles were easily

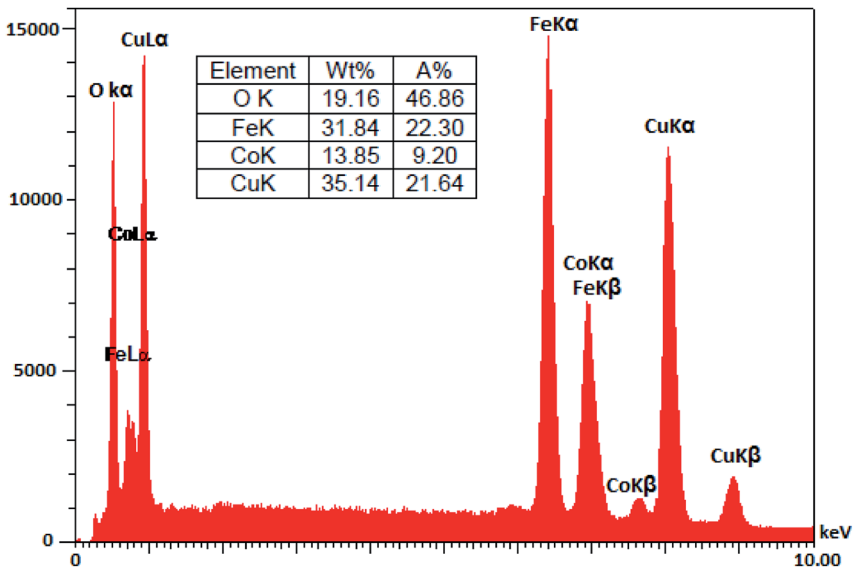

Fig. 6 EDS of $CoFe_2O_4/Cu(OH)_2$.

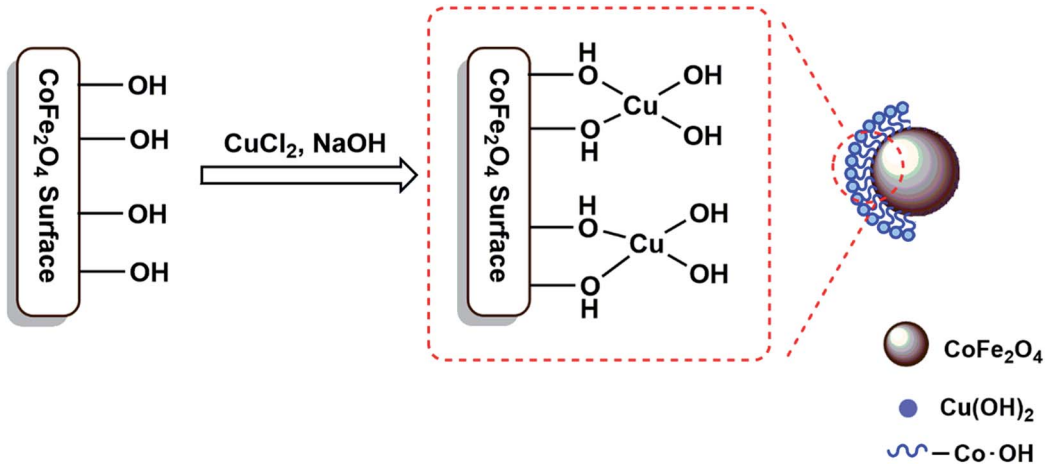

Scheme 4 Structure of $CoFe_2O_4/Cu(OH)_2$ as a surface modified nanocatalyst.

collected by an external magnet, washed several times with distilled water and ethanol and dried at 70 °C for 1 h. The recovered catalyst was reused 6 times without any significant loss of activity, under the same conditions (Fig. 7). The structure of the recovered $CoFe_2O_4/Cu(OH)_2$ nanocatalyst was confirmed using VSM, XRD, FESEM and TEM analyses after five runs (Fig. 8). Comparison of the results obtained from the recycled catalyst and the freshly prepared nanoparticles revealed that the magnetic properties, original structure and morphology of the catalyst remained unchanged after several reuses.

The hot filtration test was used for confirming the heterogeneity of as-prepared catalyst. Accordingly, the filtration of the catalyst was carried out after 30 min at 80 °C and the filtrate was allowed to react for additional 2 hours, but the reaction due to

Table 1 Nano-$CoFe_2O_4/Cu(OH)_2$-catalysed reaction of styrene oxide with phenylacetylene and sodium azide under different conditions[a]

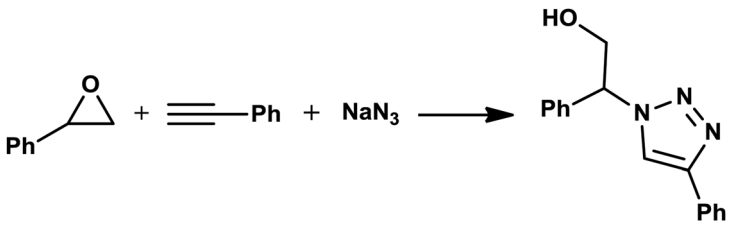

Entry	$CoFe_2O_4/Cu(OH)_2$ (g)	Solvent	Time (h)	Temperature (°C)	Yield[b] (%)
1	—	H_2O	10	60	0
2	0.01	H_2O	8	60	25
3	0.02	H_2O	8	60	55
4	0.025	H_2O	6	60	85
5	**0.032**	**H_2O**	**3.3**	**60**	**94**
6	0.04	H_2O	3	60	94
7	0.032	EtOH	4	78	50
8	0.032	CH_3CN	4	82	35
9	0.032	EtOAc	4	77	60
10	0.032	MeOH	4	65	50
11	0.032	DMF	4	100	45
12	0.032	THF	24	60	0
13	0.032	*n*-Hexane	24	68	0
14	0.032	H_2O	8	25	50
15	0.032	H_2O	5	40	65
16[c]	0.032	H_2O	5	100	Trace
17[d]	0.032	H_2O	3.5	60	90

[a] All reactions were carried out with styrene oxide (1 mmol), phenylacetylene (1 mmol) and sodium azide (1.2 mmol). [b] Isolated yields. [c] Catalysed by $CoFe_2O_4$. [d] Catalysed by $Cu(OH)_2$.

Table 2 One-pot synthesis of β-hydroxy-1,2,3-triazoles from epoxides catalyzed by nano-$CoFe_2O_4$/$Cu(OH)_2$[a]

Entry	Epoxide (a)	Alkyne	Triazole (b)	Time (h)	Yield[b] (%)
1	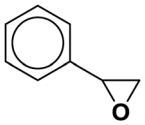	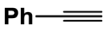	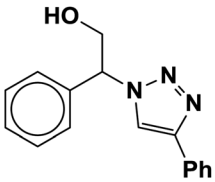	3.3	94
2	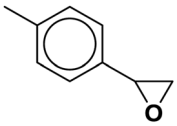	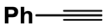	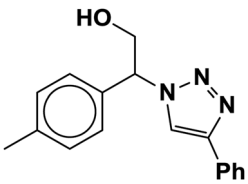	3	95
3	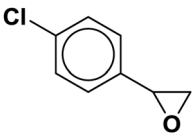	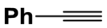	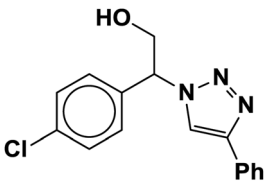	3.3	90
4	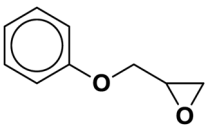	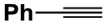	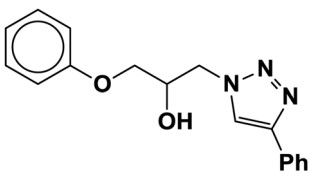	4.3	88
5	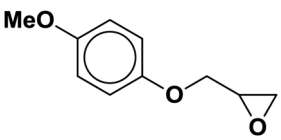	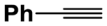	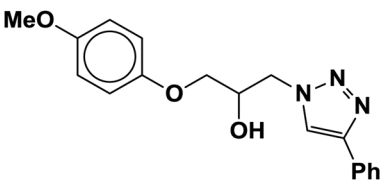	4.5	85
6	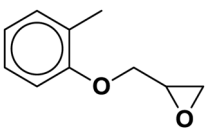	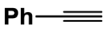	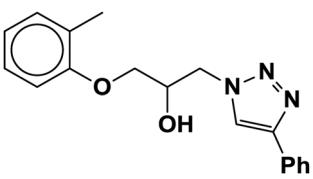	4.5	87
7	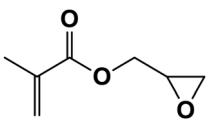	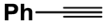	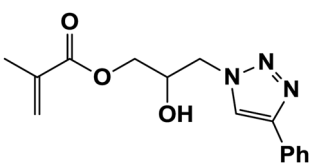	5.5	75
8	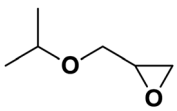	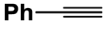	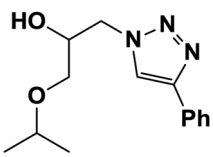	4.3	80
9	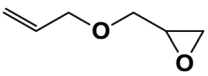	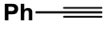	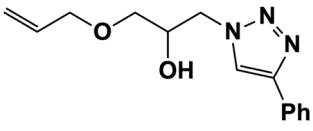	4.2	85

Table 2 (*Contd.*)

Entry	Epoxide (a)	Alkyne	Triazole (b)	Time (h)	Yield[b] (%)
10	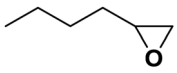		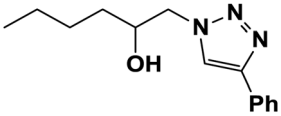	6.3	84
11	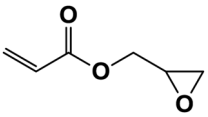		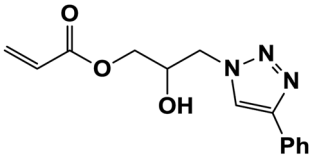	5	82
12	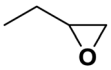		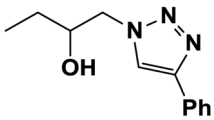	6	85
13	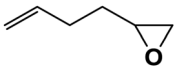		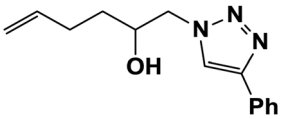	6	87
14	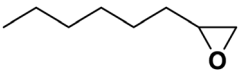		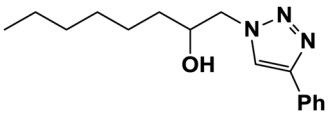	6.5	88
15	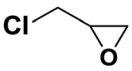		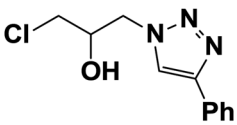	5	80
16	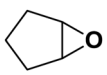		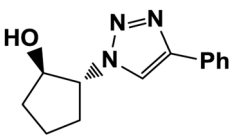	5	90
17	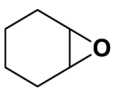		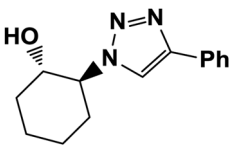	6	92
18	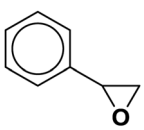	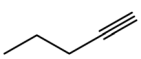	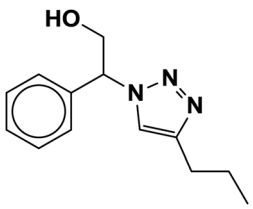	5.5	85
19	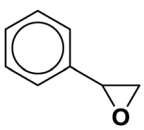	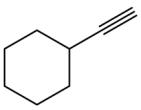	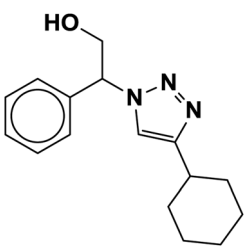	4	90

Table 2 (*Contd.*)

Entry	Epoxide (a)	Alkyne	Triazole (b)	Time (h)	Yield[b] (%)
20	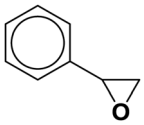	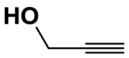	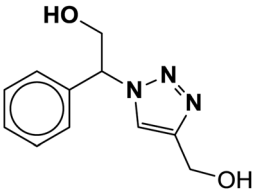	5	88
21	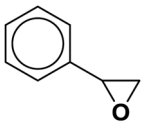	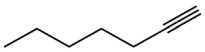	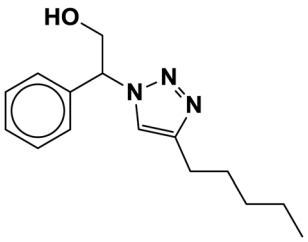	6.5	84

[a] All reactions were carried out with 1 mmol of epoxide in the presence of alkyne (1 mmol), sodium azide (1.2 mmol) and nano-$CoFe_2O_4$/$Cu(OH)_2$ (0.032 g, 0.1 mmol, 10 mol%) in water at 60 °C. [b] Yields refer to isolated pure products.

the absence of copper did not take place, and no cycloaddition reaction was occurred.

3.4. Comparison of $CoFe_2O_4$/$Cu(OH)_2$ catalytic activity with other catalysts

The comparison of the catalytic activity of the prepared $CoFe_2O_4$/$Cu(OH)_2$ nanocomposite with various catalysts in the reaction of styrene oxide, phenylacetylene and sodium azide is summarized in Table 3. As can be seen, our proposed procedure is more efficient than the other methods in terms of product yield, and it is also comparable to the most of them from viewpoints of reaction time and temperature. The study of reported literature shows that magnetic nanocatalysts have been rarely used for one-pot synthesis of 1,2,3-triazoles from epoxides (entries 2 and 3), and the overwhelming majority of the reported cases have been carried out in the presence of non-magnetic catalysts (entries 4–11). On the other hand, in some cases, the use of acid or base alongside the catalyst is essential for the reaction progress (entries 10 and 11). Therefore, our

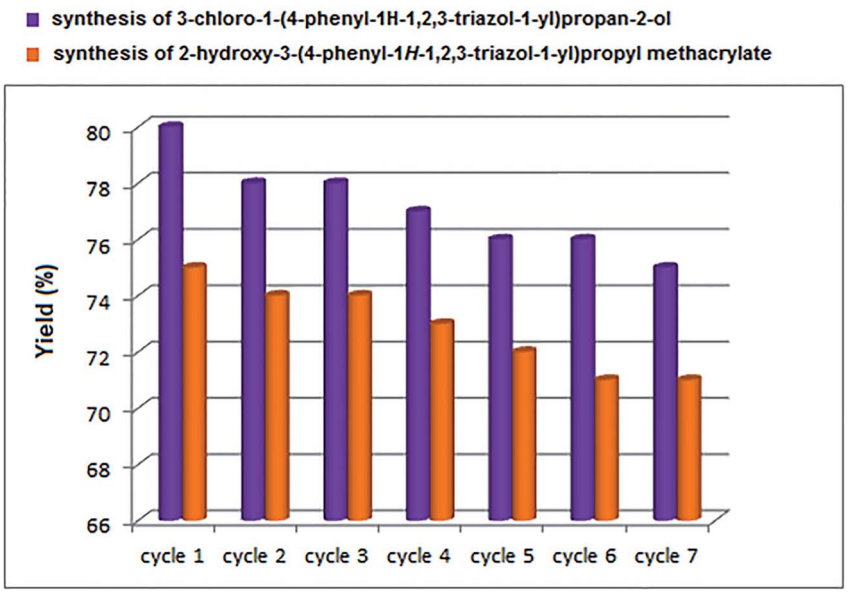

Fig. 7 Recycling of nano-$CoFe_2O_4$/$Cu(OH)_2$ in the synthesis of 3-chloro-1-(4-phenyl-1*H*-1,2,3-triazol-1-yl)propan-2-ol and 2-hydroxy-3-(4-phenyl-1*H*-1,2,3-triazol-1-yl)propyl methacrylate.

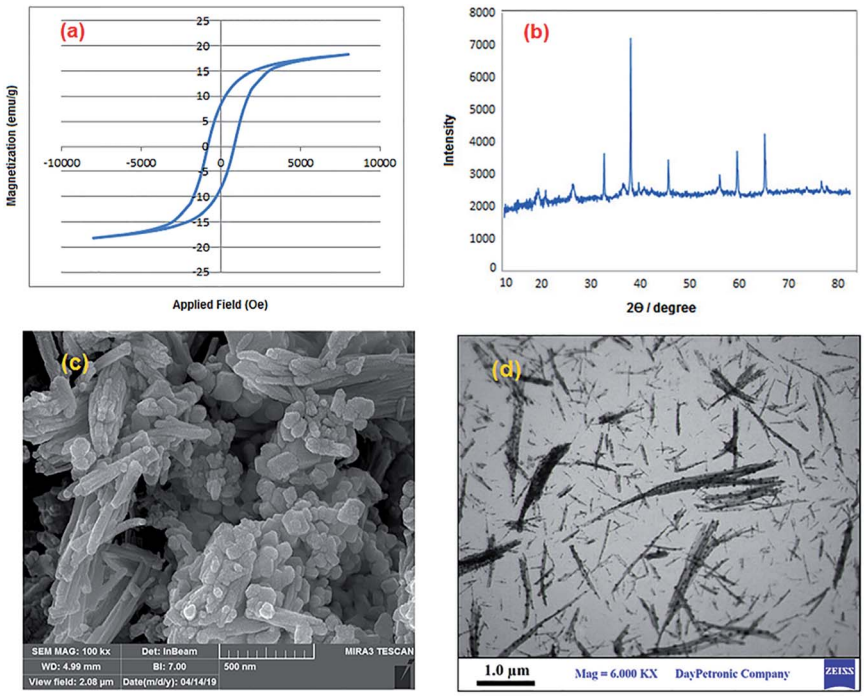

Fig. 8 (a) Magnetization curve, (b) XRD pattern, (c) FESEM and (d) TEM images of $CoFe_2O_4/Cu(OH)_2$ after five runs in the synthesis of 3-chloro-1-(4-phenyl-1*H*-1,2,3-triazol-1-yl)propan-2-ol.

method, due to the use of ferromagnetic nanocatalyst, takes advantage of both heterogeneity benefits and magnetic properties. In addition, performing of reaction in a green solvent under neutral conditions is really important privilege. Easy preparation and utilization of surface modified nanoparticles, simple separation just by an external magnet, convenient recovering, reusability after several cycles without loss of catalytic activity or magnetic property and subsequently facilitating the achievement to the goals of green chemistry are among the remarkable advantages of $CoFe_2O_4/Cu(OH)_2$ catalytic system, which highlight its importance in comparison with the most reported catalysts. Furthermore, the one-pot reaction due to the

Table 3 Comparison of $CoFe_2O_4/Cu(OH)_2$ catalytic activity with various catalysts reported for the one-pot synthesis of 2-phenyl-2-(4-phenyl-1*H*-1,2,3-triazol-1-yl)ethanol from styrene oxide, phenylacetylene and sodium azide[a]

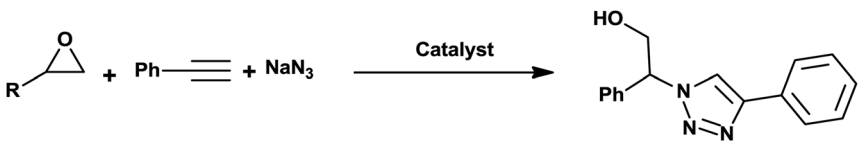

Entry	Catalyst system	NaN_3 (mmol)	Conditions	Time (h)	Yield (%)	Ref.
1	$CoFe_2O_4/Cu(OH)_2$ (10 mol%)	1.2	H_2O/60 °C	3.3	94	This work
2	Nano $CuFe_2O_4$ (10 mol%)	1.1	H_2O/60 °C	6	87	29
3	Nano Fe_2O_3 (10 mol%)	1.2	H_2O/100 °C	5	81	45
4	Cu nanoparticles/C (0.5 mol%)	1.1	H_2O/70 °C	8	93	23
5	Cu(I)@phosphorated SiO_2 (0.64 mol%)	1.1	H_2O/60 °C	1	93	30
6	Copper(I)–zeolite (8 mol%)	1.2	H_2O/r.t.	20	77	27
7	CuI (5 mol%)	1.1	PEG-400/r.t.	16	83	37
8	$CuCl_2$ (10 mol%)	1	H_2O/r.t.	5	35	31
9	$Cu(NO_3)_2 \cdot 3H_2O$ (10 mol%)	1	H_2O/r.t.	5	36.8	31
10	$[Cu(bhppda)H_2O]^b$ (5 mol%)	1.2	Ascorbic acid/H_2O/r.t.	2	90	28
11	$CuSO_4 \cdot 5H_2O$ (10 mol%)	1.2	Sodium ascorbate/H_2O/r.t.	4	92	26

[a] All reactions were carried out with styrene oxide (1 mmol) and phenylacetylene (1 mmol). [b] bhppda = N^2,N^6-bis(2-hydroxyphenyl)pyridine-2,6-dicarboxamidato dianion.

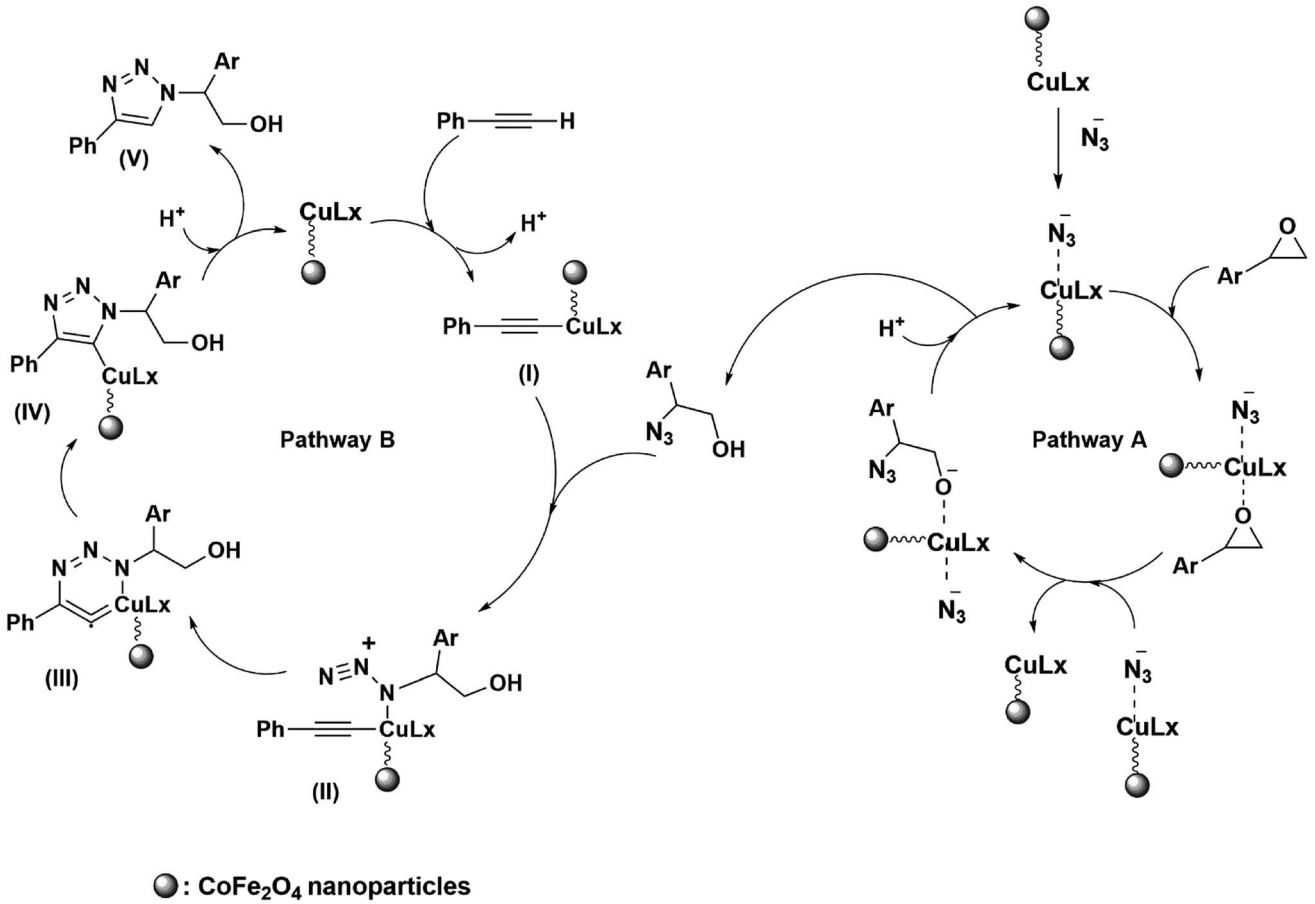

Scheme 5 Reaction mechanism proposed for the one-pot synthesis of 1,4-disubstituted β-hydroxy-1,2,3-triazole catalyzed by $CoFe_2O_4$/$Cu(OH)_2$ bifunctional catalyst.

reduction of work-up procedures and purification steps required compared to a more stepwise approach was used in order to conduct synthesis in a greener fashion.

3.5. The proposed mechanism for synthesis of 1,4-disubstituted β-hydroxy-1,2,3-triazoles catalyzed by $CoFe_2O_4$/$Cu(OH)_2$ nanocomposite

The proposed mechanism for the formation of β-hydroxy-1,4-disubstituted-1,2,3-triazoles includes two pathways (A and B) in which $CoFe_2O_4$/$Cu(OH)_2$ catalyzes both ring opening and 1,3-dipolar cycloaddition reactions.[28] The pathway A demonstrates the formation of metal azide which is followed by epoxide activation *via* $CoFe_2O_4$/$Cu(OH)_2$ catalyst. Ring opening of epoxide takes place through azide delivery from the catalyst and leads to the formation of 2-azido-2-arylethanol. The regioselective cleavage of oxiranes carrying alkyl and allyl substituents by azide ion is strongly favored from less hindered carbon of the epoxide ring *via* S_N2 type of mechanism (β-cleavage); however, aryl-substituted epoxides prefer to be opened from the more sterically hindered position *via* S_N1 type of mechanism (α-cleavage).

The pathway B displays the insertion of copper catalyst to the C–H bond of terminal alkyne in order to activate the phenylacetylene and produce the intermediate (I), which facilitates the [3 + 2] cycloaddition between carbon–carbon triple bond of the 2-azido-2-arylethanol and *in situ* generated intermediate (II), to give the Cu–C-triazole (IV). The alkyne consumption and also the generation and the disappearance of the 2-azido-2-alkylethanol intermediate, were monitored by gas chromatography (GC) analysis and thin layer chromatography (TLC) runs of the reaction mixture. Finally, protonolysis of the Cu–C bond of intermediate (IV) by aqueous media affords the corresponding β-hydroxy-1,2,3-triazole (V) (Scheme 5).

4. Conclusions

In summary, the magnetic nanocatalyst of $CoFe_2O_4$/$Cu(OH)_2$ has been successfully prepared through a simple method and it was then characterized using various techniques such as FESEM, EDS, TEM, XRD, VSM and FT-IR. This novel composite has been demonstrated to be an efficient catalyst for one-pot synthesis of a wide variety of 1,4-disubstituted-1,2,3-triazoles *via* three component reactions of sodium azide, terminal alkyne, and different epoxides in water. The simple procedure, short reaction times, perfect regioselectivity, high product yields, the use of benign solvent, easy separation of catalyst using an external magnet and efficient recycling are remarkable

aspects of this proposed protocol that make it to be an important addition to the existing methodologies for synthesis of 1,4-disubstituted-1,2,3-triazoles.

Conflicts of interest

There are no conflicts to declare.

Acknowledgements

The financial support of this work by the Research Council of Payame Noor University is gratefully acknowledged.

References

1 M. Whitting, J. Muldoon, Y. C. Lin, S. M. Silverman, W. Lindstrom, A. J. Olson, H. C. Kolb, M. G. Finn, K. B. Sharpless, J. H. Elder and V. V. Fokin, *Angew. Chem., Int. Ed.*, 2006, **45**, 1435.
2 B. S. Holla, M. Mahalinga, M. S. Karthikeyan, B. Poojary, P. M. Akberali and N. S. Kumari, *Eur. J. Med. Chem.*, 2005, **40**, 1173.
3 V. Pande and M. J. Ramos, *Bioorg. Med. Chem. Lett.*, 2005, **15**, 5129.
4 W. Q. Fan and A. R. Katritzky, in *Comprehensive Heterocyclic Chemistry II*, ed. A. R. Katritzky, C. W. Rees and E. F. Scriven, Elsevier Science, Oxford, 1996, vol. 4, p. 1.
5 A. Kamal, S. Prabhakar, M. J. Ramaiah, P. V. Reddy, Ch. R. Reddy, A. Mallareddy, N. Shankaraiah, T. L. N. Reddy, S. N. C. V. L. Pushpavalli and M. Pal-Bhadra, *Eur. J. Med. Chem.*, 2011, **46**, 3820.
6 F. C. Silva, M. C. B. V. de Souza, I. I. P. Frugulhetti, H. C. Castro, S. L. d. O. Souza, T. M. L. de Souza, D. Q. Rodrigues, A. M. T. Souza, P. A. Abreu, F. Passamani, C. R. Rodrigues and V. F. Ferreira, *Eur. J. Med. Chem.*, 2009, **44**, 373.
7 S. Palhagen, R. Canger, O. Henriksen, J. A. van Parys, M.-E. Riviere and M. A. Karolchyk, *Epilepsy Res.*, 2001, **43**, 115.
8 J. N. Sangshetti, R. R. Nagawade and D. B. Shinde, *Bioorg. Med. Chem. Lett.*, 2009, **19**, 3564.
9 G. Ravi, A. R. Nath, A. Nagaraj, S. Damodhar and G. N. Rao, *Der Pharma Chem.*, 2014, **6**, 223.
10 C. Menendez, A. Chollet, F. Rodriguez, C. Inard, M. R. Pasca, C. Lherbet and M. Baltas, *Eur. J. Med. Chem.*, 2012, **52**, 275.
11 T. W. Kim, Y. Yong, S. Y. Shin, H. Jung, K. H. Park, Y. H. Lee, Y. Lim and K. Y. Jung, *Bioorg. Chem.*, 2015, **59**, 1.
12 R. Raj, P. Singh, P. Singh, J. Gut, P. J. Rosenthal and V. Kumar, *Eur. J. Med. Chem.*, 2013, **62**, 590.
13 M. F. Mady, G. E. A. Awad and K. B. Jørgensen, *Eur. J. Med. Chem.*, 2014, **84**, 433.
14 A. Domling and I. Ugi, *Angew. Chem., Int. Ed.*, 2000, **39**, 3168.
15 R. Huisgen, *Pure Appl. Chem.*, 1989, **61**, 613.
16 R. Huisgen, G. Szeimies and L. Moebius, *Chem. Ber.*, 1965, **98**, 4014.
17 C. S. Radatz, L. d. A. Soares, E. F. Vieira, D. Alves, D. Russowsky and P. H. Schneider, *New J. Chem.*, 2014, **38**, 1410.
18 M. I. Mangione, R. A. Spanevello and M. B. Anzardi, *RSC Adv.*, 2017, **7**, 47681.
19 H. X. Siyang, H. L. Liu, X. Y. Wu and P. N. Liu, *RSC Adv.*, 2015, **5**, 4693.
20 W. D. Castro-Godoy, A. A. Heredia, L. C. Schmidt and J. E. Arguello, *RSC Adv.*, 2017, **7**, 33967.
21 N. V. Sokolova and V. G. Nenajdenko, *RSC Adv.*, 2013, **3**, 16212.
22 W. Yang, T. Miao, P. Li and L. Wang, *RSC Adv.*, 2015, **5**, 95833.
23 F. Alonso, Y. Moglie, G. Radivoy and M. Yus, *J. Org. Chem.*, 2011, **76**, 8394.
24 F. Alonso, Y. Moglie, G. Radivoy and M. Yus, *Adv. Synth. Catal.*, 2010, **352**, 3208.
25 H. Sharghi, M. H. Beyzavi, A. Safavi, M. M. Doroodmand and R. Khalifeh, *Adv. Synth. Catal.*, 2009, **351**, 2391.
26 J. S. Yadav, B. V. S. Reddy, G. M. Reddy and D. N. Chary, *Tetrahedron Lett.*, 2007, **48**, 8773.
27 T. Boningari, A. Olmos, B. M. Reddy, J. Sommer and P. Pale, *Eur. J. Org. Chem.*, 2010, **2010**, 6338.
28 H. Sharghi, M. Hosseini-Sarvari, F. Moeini, R. Khalifeh and A. S. Beni, *Helv. Chim. Acta*, 2010, **93**, 435.
29 B. S. P. Anil Kumar, K. Harsha Vardhan Reddy, G. Satish, R. Uday Kumar and Y. V. D. Nageswar, *RSC Adv.*, 2014, **4**, 60652.
30 H. Naeimi and V. Nejadshafiee, *New J. Chem.*, 2014, **38**, 5429.
31 K. Rajender Reddy, C. Uma Maheswari, K. Rajgopal and M. Lakshmi Kantam, *Synth. Commun.*, 2008, **38**, 2158.
32 H. Esmaeili-Shahri, H. Eshghi, J. Lari and S. A. Rounaghi, *Appl. Organomet. Chem.*, 2018, **32**, e3947.
33 N. Noshiranzadeh, M. Emami, R. Bikas and A. Kozakiewicz, *New J. Chem.*, 2017, **41**, 2658.
34 H. Sharghi and I. Ghaderi, *Org. Chem. Res.*, 2017, **3**, 162.
35 H. Sharghi, A. Khoshnood, M. M. Doroodmand and R. Khalifeh, *J. Iran. Chem. Soc.*, 2012, **9**, 231.
36 H. Sharghi, S. Ebrahimpourmoghaddam, M. M. Doroodmand and A. Purkhosrow, *Asian J. Org. Chem.*, 2012, **1**, 377.
37 G. Kumaraswamy, K. Ankamma and A. Pitchaiah, *J. Org. Chem.*, 2007, **72**, 9822.
38 J. Lu, E. Q. Ma, Y. H. Liu, Y. M. Li, L. P. Mo and Z. H. Zhang, *RSC Adv.*, 2015, **5**, 59167.
39 D. B. Ramachary, A. B. Shashank and S. Karthik, *Angew. Chem., Int. Ed.*, 2014, **53**, 1.
40 D. B. Ramachary, K. Ramakumar and V. V. Narayana, *Chem.–Eur. J.*, 2008, **14**, 9143.
41 Z. E. Blastik, B. Klepetářová and P. Beier, *ChemistrySelect*, 2018, **3**, 7045.
42 R. Sangwan, Javed, A. Dubey and P. K. Mandal, *ChemistrySelect*, 2017, **2**, 4733.
43 H. Yuan, L. Zhang, Z. Liu, Y. Liu, J. Wang and W. Li, *Org. Biomol. Chem.*, 2017, **15**, 4286.
44 F. Nasiri, A. Zolali and S. Asadbegi, *J. Heterocycl. Chem.*, 2016, **53**, 989.

45 M. Murty, M. R. Katiki and D. Kommula, *Can. Chem. Trans.*, 2016, **4**, 47.
46 C. W. Lim and I. S. Lee, *Nano Today*, 2010, **5**, 412.
47 M. Gawande, A. Rathi, P. Branco and R. Varma, *Appl. Sci.*, 2013, **3**, 656.
48 Z. Zhang, Y. Liu, G. Yao, G. Zu and Y. Hao, *Int. J. Appl. Ceram. Technol.*, 2013, **10**, 142.
49 A. H. Lu, E. L. Salabas and F. Schuth, *Angew. Chem., Int. Ed.*, 2007, **46**, 1222.
50 Y. Zhu, L. P. Stubbs, F. Ho, R. Liu, C. P. Ship, J. A. Maguire and N. S. Hosmane, *ChemCatChem*, 2010, **2**, 365.
51 T. Wang, L. Zhang, H. Wang, W. Yang, Y. Fu, W. Zhou, W. Yu, K. Xiang, Z. Su, S. Dai and L. Chai, *ACS Appl. Mater. Interfaces*, 2013, **5**, 12449.
52 J. Saiz, E. Bringas and I. Ortiz, *J. Chem. Technol. Biotechnol.*, 2014, **89**, 909.
53 B. Chen, Z. Zhu, J. Ma, M. Yang, J. Hong, X. Hu, Y. Qiu and J. Chen, *J. Colloid Interface Sci.*, 2014, **434**, 9.
54 V. Polshettiwar, R. Luque, A. Fihri, H. Zhu, M. Bouhrara and J.-M. Basset, *Chem. Rev.*, 2011, **111**, 3036.
55 Z. Shokri, B. Zeynizadeh and S. A. Hosseini, *J. Colloid Interface Sci.*, 2017, **485**, 99.
56 K. Bakhmutsky, N. L. Wieder, M. Cargnello, B. Galloway, P. Fornasiero and R. J. Gorte, *ChemSusChem*, 2012, **5**, 140.
57 R. G. Chaudhuri and S. Paria, *Chem. Rev.*, 2012, **112**, 2373.
58 S. Hassanzadeh, R. Eisavi and M. Abbasian, *Appl. Organomet. Chem.*, 2018, **32**, e4520.
59 R. Eisavi and S. Alifam, *Phosphorus, Sulfur Silicon Relat. Elem.*, 2017, **193**, 211.
60 R. Eisavi, S. Ghadernejad, B. Zeynizadeh and F. M. Aminzadeh, *J. Sulfur Chem.*, 2016, **37**, 537.
61 R. Eisavi, F. Ahmadi, B. Ebadzade and S. Ghadernejad, *J. Sulfur Chem.*, 2017, **38**, 614.
62 S. Hassanzadeh, R. Eisavi and M. Abbasian, *J. Sulfur Chem.*, 2019, **40**, 240.
63 M. Mahmoudzadeh, E. Mehdipour and R. Eisavi, *J. Coord. Chem.*, 2019, **72**, 841.
64 Z. P. Sun, L. Liu, D. Z. Jia and W. Pan, *Sens. Actuators, B*, 2007, **125**, 144.
65 S. Sathiya, K. Parasuraman, M. Anbarasu and K. Balamurugan, *Nano Vision*, 2015, **5**, 133.
66 J. M. Aguirre, A. Gutiérrezb and O. iraldo, *J. Braz. Chem. Soc.*, 2011, **22**, 546.
67 H. Iida, K. Takayannagi, T. Nakamishi and T. Osaka, *J. Colloid Interface Sci.*, 2007, **314**, 274.
68 L. Wang, K. Zhang, Z. Hu, W. Duan, F. Cheng and J. Chen, *Nano Res.*, 2014, **7**, 199.